Physical Modelling of Complex Systems: Assignment 9: The Brusselator Model

Thibeau Wouters

May 24, 2021

Contents

In this exercise on pattern formation and Turing instabilities, we will consider the Brusselator model, a toy-model for the Belousov-Zhabotinsky reaction. The differential equations of the Brusselator are given by

$$\frac{\partial u}{\partial t} = a - (b+1)u + u^2 v + D_u \frac{\partial^2 u}{\partial x^2} \tag{1}$$

$$\frac{\partial v}{\partial t} = bu - u^2 v + D_v \frac{\partial^2 v}{\partial x^2}\,, \tag{2}$$

and we set the parameters equal to $a = 1.5$, $D_u = 2.8$ and $D_v = 22.4$ below. We follow the general approach presented during the lecture (or in Chapter 2 of *Mathematical Biology* by Murray [1]) and non-dimensionalize the above equations. For this, we introduce a characteristic length-scale L for the problem, and set

$$\gamma \equiv \frac{L^2}{D_u}, \quad t^* \equiv \frac{1}{\gamma} t, \quad x^* = \frac{x}{L}, \quad d = \frac{D_v}{D_u}\,. \tag{3}$$

Note that for general systems, γ also contains a rate such that it has a dimension of time, but in our reactions, the rates are equal to one. The above equations become

$$\frac{\partial u}{\partial t^*} = \gamma(a - (b+1)u + u^2 v) + \frac{\partial^2 u}{\partial (x^*)^2} \equiv \gamma f(u,v) + \frac{\partial^2 u}{\partial (x^*)^2} \tag{4}$$

$$\frac{\partial v}{\partial t^*} = \gamma(bu - u^2 v) + d\frac{\partial^2 v}{\partial (x^*)^2} \qquad \equiv \gamma g(u,v) + d\frac{\partial^2 v}{\partial (x^*)^2}\,. \tag{5}$$

Below, we will drop the asterisks in these equations for notational simplicity.

1 Homogeneous steady state solutions

We first calculate the homogeneous steady state (HSS) solutions, which means we set $D_u = 0 = D_v$, and set both equations above equal to zero. This gives the system of equations

$$\begin{cases} a - (b+1)u + u^2 v & = 0 \\ u(b - uv) & = 0\,. \end{cases} \tag{6}$$

If $u = 0$, then the first equation gives $a = 0$, which is not possible. Hence the second equation gives $uv = b$, and the first equation becomes

$$a - (b+1)u + b = a - u = 0\,, \tag{7}$$

such that the homogeneous steady state solution is unique and given by

$$(u_0, v_0) = \left(a, \frac{b}{a}\right)\,. \tag{8}$$

The Jacobian for the homogeneous system is

$$J(u,v) = \begin{pmatrix} -(b+1)+2uv & u^2 \\ b-2uv & -u^2 \end{pmatrix}, \tag{9}$$

such that the Jacobian evaluated at the HSS is

$$J \equiv J(u_0,v_0) = \begin{pmatrix} b-1 & a^2 \\ -b & -a^2 \end{pmatrix} \equiv \begin{pmatrix} f_u & f_v \\ g_u & g_v \end{pmatrix}, \tag{10}$$

where we have defined f_u to be the u-derivative of function f evaluated at the HSS et cetera. This implies we have to require

$$\operatorname{tr} J(u_0,v_0) = b-1-a^2 < 0, \quad \det J(u_0,v_0) = a^2 > 0\,, \tag{11}$$

such that the HSS is stable, as required in the theory of pattern formation in reaction-diffusion systems. Note that the condition on the trace restricts b to $b < 1+a^2$, while the determinant condition is certainly satisfied.

We can interpret u and v to represent the concentrations of two morphogens A and B. If we want to have pattern formation, we should have $J_{11} > 0$ and $J_{22} < 0$, which gives the additional constraint $b > 1$. Hence A is an activator and B a repressor, and B diffuses faster compared to A. The situation now resembles local activation and long range inhibition. From the lecture, we know that this type of system is able to produce patterns from diffusion-driven instabilities, which we will now explore.

2 Turing instability

As seen during the lecture, patterns can evolve from a diffusion driven instability (*Turing instability*) under certain conditions. This means that the HSS becomes unstable once we consider the full reaction diffusion system. Defining

$$\mathbf{w} = \begin{pmatrix} u-u_0 \\ v-v_0 \end{pmatrix}, \tag{12}$$

the linearisation is

$$\frac{\partial \mathbf{w}}{\partial t} = \gamma J\mathbf{w} + D\nabla^2\mathbf{w}\,, \quad D = \begin{pmatrix} 1 & 0 \\ 0 & d \end{pmatrix}. \tag{13}$$

Now, let $\mathbf{W}$ be the solution of the time-independent eigenvalue equation

$$\nabla^2\mathbf{W} + k^2\mathbf{W} = 0\,, \tag{14}$$

with eigenvalue k, and suppose the solution satisfies no-flux boundary conditions. This is chosen such that the system has no external input and the observed patterns are showing

self-organisation in the system. Since we are linearising around the HSS, the general solution is given by the sum

$$\mathbf{w} = \sum_k c_k e^{\sigma_k t} \mathbf{W}_k \,, \tag{15}$$

where σ_k is the *growth rate*. The growth rates are the eigenvalues of the matrix $\gamma J - k^2 D$, which is

$$\gamma J - k^2 D = \begin{pmatrix} \gamma f_u - k^2 & \gamma f_v \\ \gamma g_u & \gamma g_v - d k^2 \end{pmatrix} \,, \tag{16}$$

so the σ_k are roots of the characteristic polynomial

$$\det\left(\gamma J - k^2 D - \sigma_k\right) = 0 \,. \tag{17}$$

The characteristic polynomial is

$$\sigma_k^2 + \left[k^2(1+d) - \gamma(f_u + g_v)\right] \sigma_k + h(k^2) = 0 \,, \tag{18}$$

where $h(k^2)$ is the polynomial

$$h(k^2) = d k^4 - \gamma(d f_u + g_v) k^2 + \gamma^2 \det J \,. \tag{19}$$

If we fill in the results that we obtained for the Brusselator model, this polynomial becomes

$$h(k^2) = d k^4 - \gamma(d(b-1) - a^2) k^2 + \gamma^2 a^2 \,. \tag{20}$$

Since morphogenesis requires that the HSS becomes unstable if diffusion is taken into account, we require that equation (18) has at least one solution with positive real part. This is possible if (i) the coefficient in front of σ_k in the characteristic polynomial is negative for some $k \neq 0$, or (ii) if $h(k^2) < 0$ for some $k \neq 0$. However, (i) can never occur, since this coefficient is always positive (recall that $f_u + g_v < 0$ as we required that the HSS is stable if diffusion is neglected) and so (ii) must be fulfilled. Since $h(k^2)$ is a parabola, the function becomes negative first at the minimum of $h(k^2)$, which is

$$k_m^2 = \gamma \frac{d f_u + g_v}{2d} = \gamma \frac{d(b-1) - a^2}{2d} \,. \tag{21}$$

Since this must be positive, we also deduce the requirement $d f_u + g_v > 0$. Together with the constraint that $f_u + g_v < 0$ found earlier, the range of b is restricted to

$$1 + \frac{a^2}{d} < b < 1 + a^2 \,. \tag{22}$$

The minimum of h is by definition equal to $h(k_m^2)$ and hence

$$h_{\min} = \gamma^2 \left[\det J - \frac{(d f_u + g_v)^2}{4d}\right] \,. \tag{23}$$

At the bifurcation point, when $h_{\min} = 0$, this equation gives

$$\det J = \frac{(df_u + g_v)^2}{4d}\,, \tag{24}$$

and this allows us to determine the critical value b_c for the bifurcation parameter. For the Brusselator model, equation (24) becomes

$$a^2 = \frac{(d(b-1) - a^2)^2}{4d}\,, \tag{25}$$

which gives the following quadratic polynomial in b

$$d^2b^2 - 2d(d + a^2)b + (d - a^2)^2 = 0\,. \tag{26}$$

There are two solutions, namely

$$b_\pm = \frac{d + a^2 \pm \sqrt{(d + a^2)^2 - (d - a^2)^2}}{d} = \left(1 \pm \frac{a}{\sqrt{d}}\right)^2\,. \tag{27}$$

However, due to the restrictions on b, only one solution is kept. Indeed, expanding the square, we find

$$b_\pm = 1 + \frac{a^2}{d} \pm \frac{2a}{\sqrt{d}}\,, \tag{28}$$

such that b_- does not lie in the allowed range for b. We conclude that

$$b_c = \left(1 + \frac{a}{\sqrt{d}}\right)^2 \tag{29}$$

is the critical value for the bifurcation parameter. The critical wavelength is

$$k_c^2 \equiv k_m^2(b = b_c) = \gamma\frac{d\left[(\sqrt{d} + a)^2 - 1\right] - a^2}{2d} \tag{30}$$

We can verify the numerical calculations graphically. Using the values of the parameters mentioned in the beginning, we get $b_c = 2.3419$ and b is restricted to the range $1.2813 \leq b \leq 3.25$. The critical wavelength squared depends on γ in our calculations above, and for $\gamma = 1$ (which is the value for γ we use in the two plots below) is equal to $k_c^2 = 0.5303$. For example, in Figure 1, we plot the functions $h(k^2)$. The figure clearly shows that the graph crosses the k^2-axis at the critical value b_c, and has a zero at the critical wavelength squared. Figure 2 shows that at the bifurcation point, a range of wavelengths become unstable. This is indeed the predicted Turing instability from above.

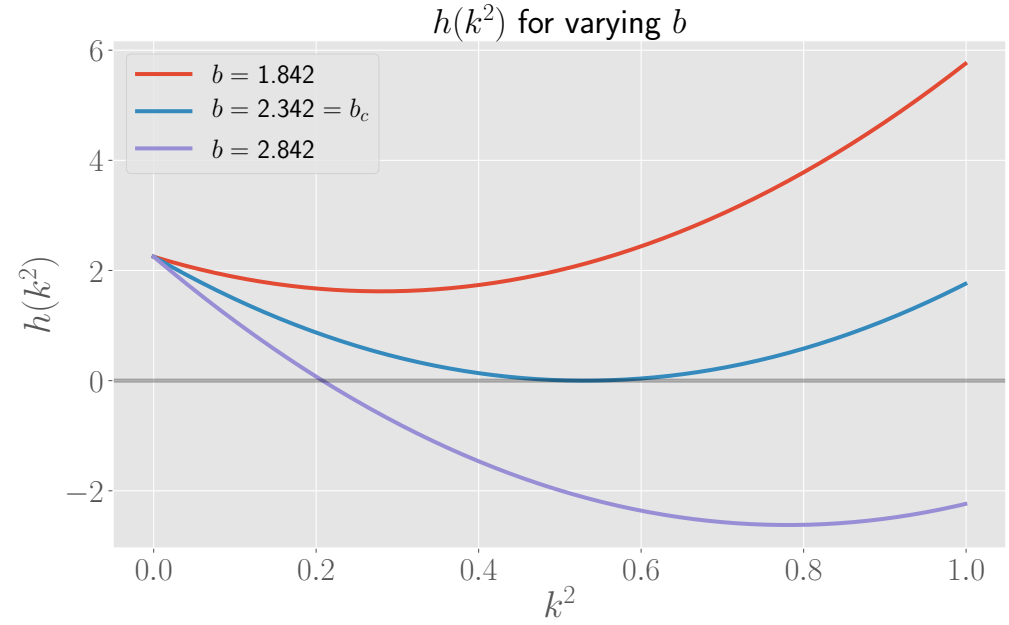

Figure 1: Plots of the functions $h(k^2)$, for varying values of b. Above the critical value b_c, the parabola becomes negative for a certain range.

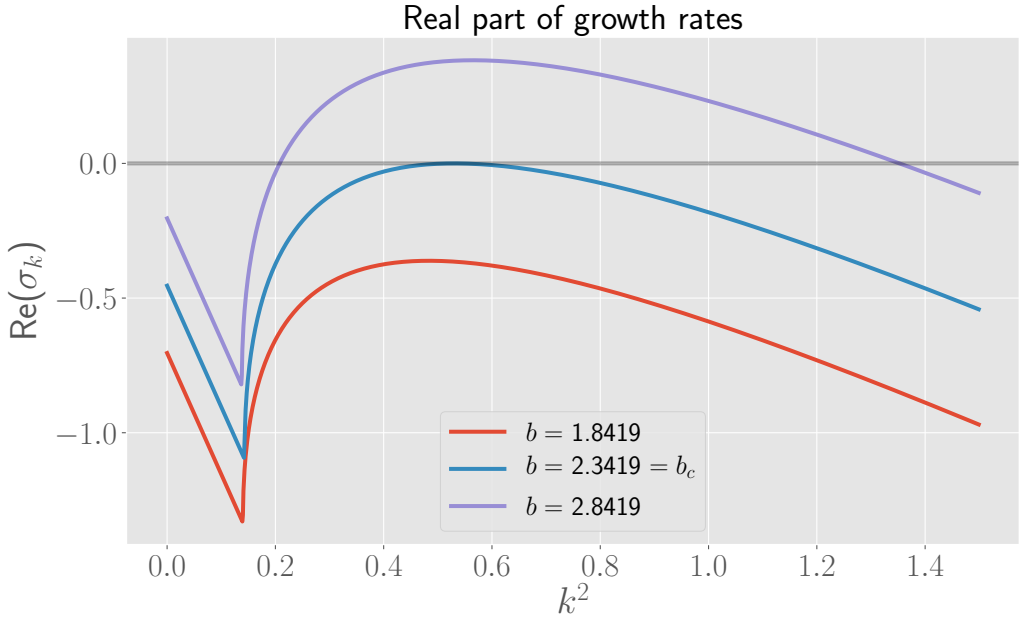

Figure 2: Real part of the growth rates σ_k. Above the bifurcation point $b = b_c$, a range of the wavelengths becomes unstable.

3 Spatiotemporal dynamics

We investigate the behaviour of the system while varying the bifurcation parameter b, the initial condition and the domain size L. We let the domain of x be of the form $[0, L]$ and work with no-flux boundary conditions. One initial condition we explore is the sine wave perturbation, where a wave-like perturbation is added on top of the HSS. Because of the boundary conditions, the wave should have the form

$$u_{\text{in}}(x) = a + A\cos\left(\frac{n\pi x}{L}\right), \quad n \in \mathbb{Z}, \tag{31}$$

where A gives the amplitude of the perturbation and is assumed to be small compared to the HSS. A similar initial condition holds for v, with a replaced by b/a. Another initial condition we explore is white noise. Here, one draws random numbers from a certain distribution and adds these as perturbation on top of the HSS. We choose for a Gaussian distribution with mean zero and standard deviation A (again characterizing the 'strength' of the perturbation and assumed to be small compared to the HSS).

To perform the numerical integration, we have chosen to adapt the code written for assignment 8 to be able to solve two component systems, such as the model currently considered. However, given that the discretization of space and time must be fine enough to reduce errors during the calculations, which also implies a larger computational cost, using a built-in solver of Python could make the calculations more precise and faster. Nevertheless, Figure 3 clearly shows that the system indeed exhibits pattern formation at late times (the figure uses $b = b_c + 0.1$ and $t = 5$) and so we conclude that our solver is adequate for the current problem.

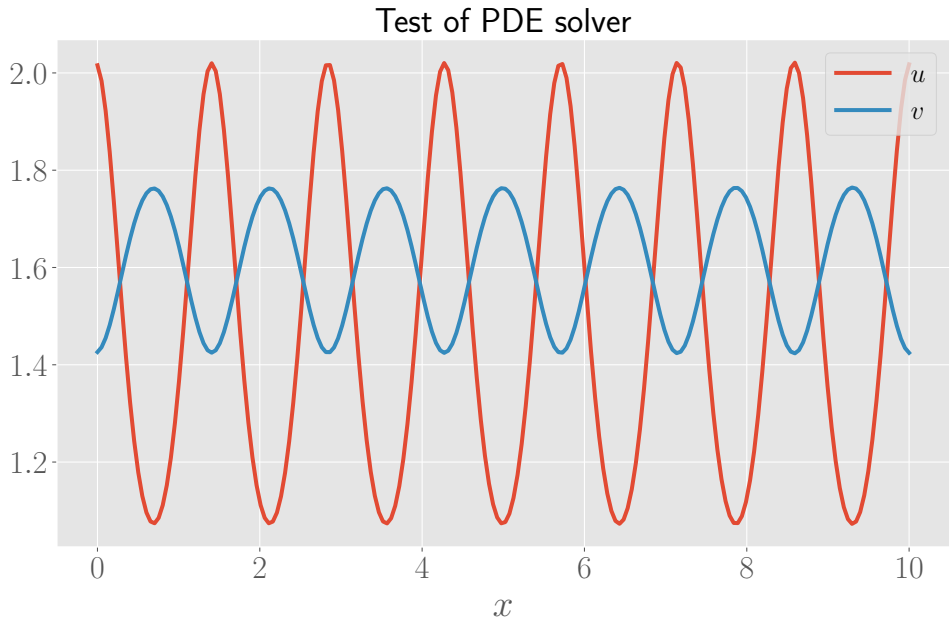

Figure 3: Test of the PDE solver written for this assignment, with $b = b_c + 0.1$. The system clearly self-organizes into a pattern formation.

Figure 3 also shows the type of pattern that the system develops. Maxima of u and minima of v are located at the same points and vice versa. This type of pattern is characteristic of a Jacobian (for the homogeneous system) with sign pattern

$$\begin{pmatrix} + & + \\ - & - \end{pmatrix}, \tag{32}$$

which is indeed the sign pattern of our Jacobian matrix. The other case, where the signs of the off-diagonal parts are swapped, has a pattern where the maxima (and minima) of u and v are aligned with each other [1, p.88].

The wavelength of the pattern can be estimated from the graph and gives $\omega \approx 1.4$. We can compute the critical wavelength, which is defined as $\omega_c = 2\pi/k_c$. For $b = b_c + 0.1$ and using $L = 10$ in the definition of γ, this gives $\omega_c \approx 1.3801$ which agrees with the above plot.

In the exploration of the dynamics below, the red curve will denote the concentration of u, and the blue curve the concentration of v, as in Figure 3. We will integrate the solutions until time $t = 5$ and by default set $L = 10$ and $b = b_c + 0.1$ and use the sine wave perturbation with $n = 1$ as initial condition. This initial condition can be seen as a disturbance due to a travelling wave inside the system which initiates the pattern formation, since the shape of this initial condition resembles a travelling wave, as seen in Figure 4. As the above example shows, $t = 5$ can be considered a 'late time' for this system, meaning that, if the conditions permit it, patterns are already formed at this timescale. Of course, these can change depending on which variation is performed.

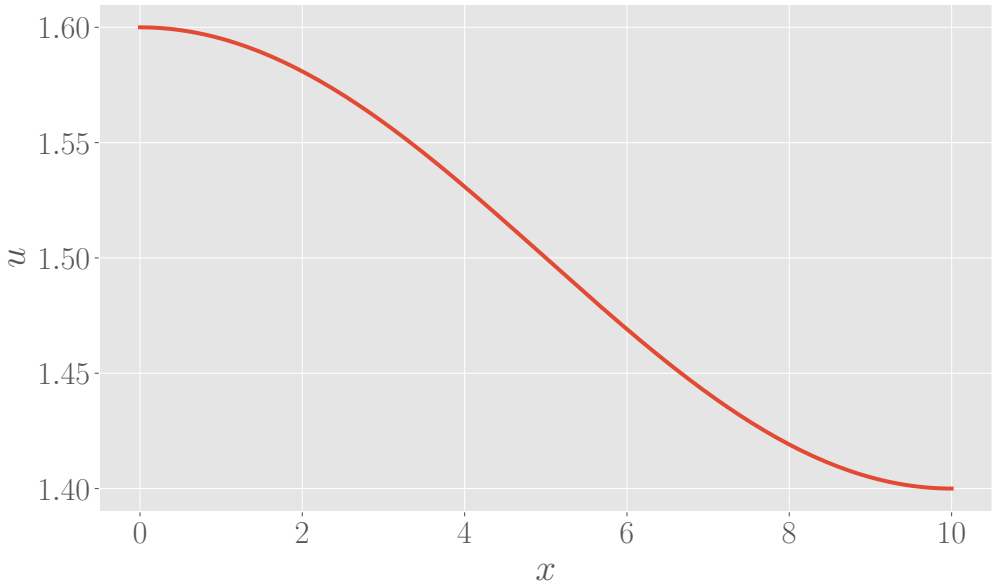

Figure 4: Sine wave perturbation for u (with HSS $u_0 = a = 1.5$) as initial condition, with $n = 1$. The shape resembles a travelling wave, which disturbs the system and initiates the pattern formation

3.1 Varying b

We vary the bifurcation parameter b, with values $b = 1.5, 2, 2.5$ and 3: the first two values are below b_c, while the other two are above b_c. The result is shown in Figure 5. As expected, when b is below the critical value, all wavelengths are stable and perturbations die out over time and at late times, the solutions tend towards the HSS. When b is above the critical value, the perturbations evolve towards a pattern.

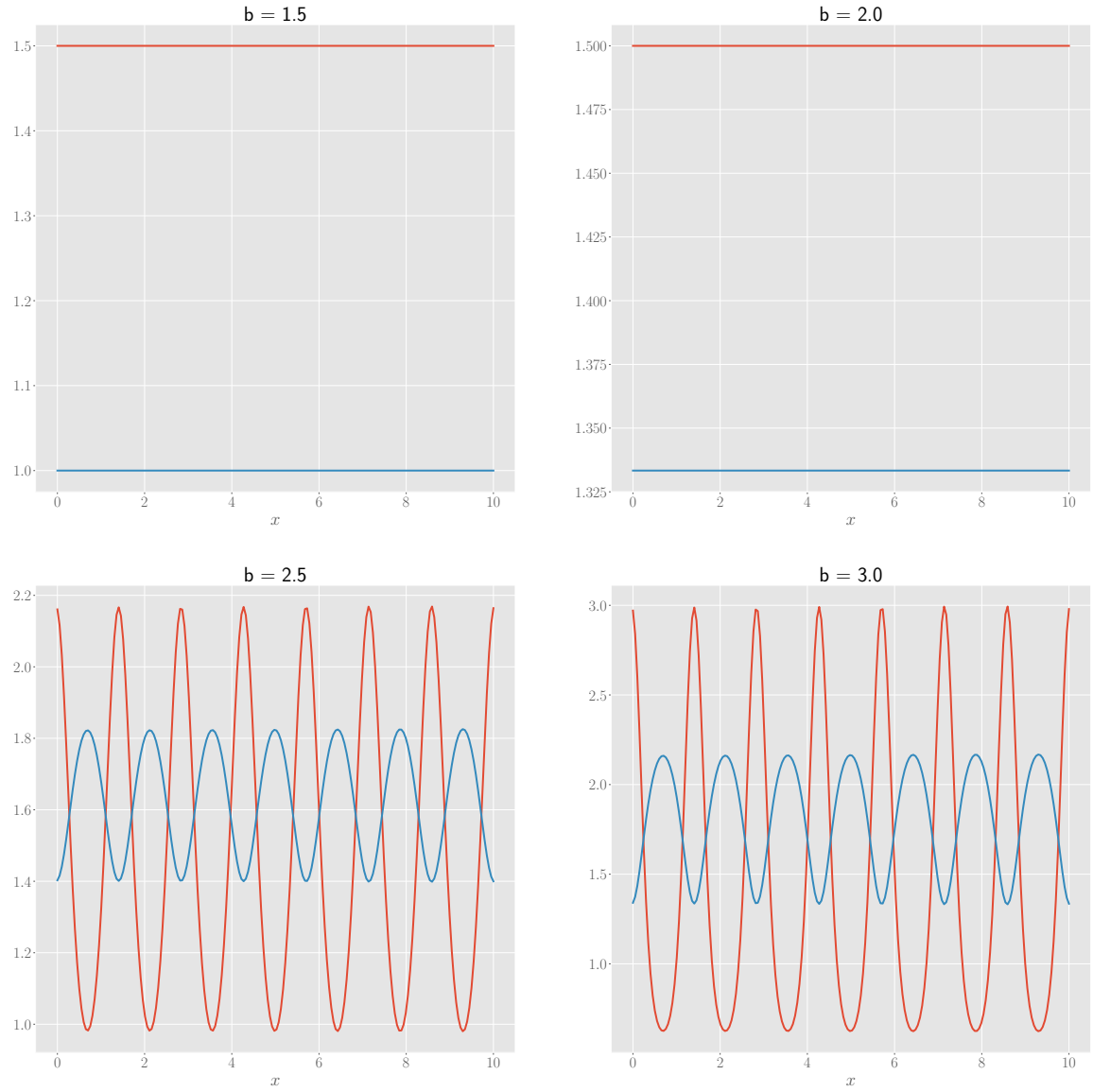

Figure 5: Varying the parameter b in the model.

3.2 Varying initial condition

We now look at the effect of varying the initial conditions. Above, we presented two possible initial conditions: sine waves and white noise. Both will be discussed and varied. For the sine waves, we can play around with the integer n from equation (31), which essentially determines the amount of wavelengths that fit in the domain. For the white noise perturbations, we will vary the amplitude of the perturbation A.

The variation of sine wave initial conditions is shown in Figure 6. Overall, it appears as

if this does not change the pattern much. The values at the boundaries can change (either a local maximum or local minimum), but the wavelength of the pattern does not change much. The amplitudes of the pattern do not change when n is varied. For $n = 25$, not all peaks of the pattern have an equal height, although it is difficult to know the cause behind this. It is likely that this is the result of computational errors and could be integrated out at later times. We conclude that the system is very stable against the variation of n in the initial condition.

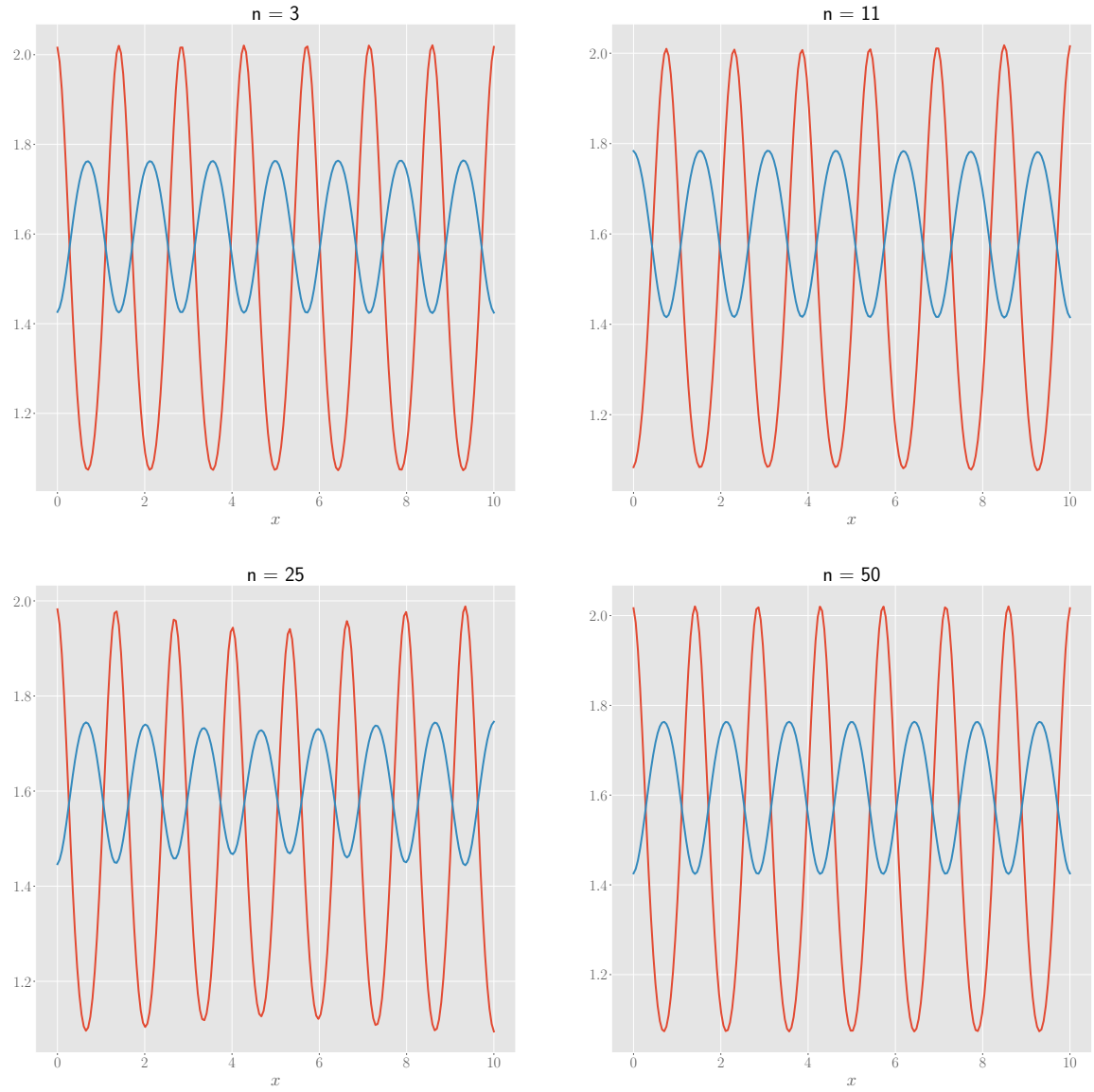

Figure 6: Varying n in the initial condition of sine wave perturbations.

The variation of the amplitude of white noise is shown in Figure 7. Essentially the same discussion as above can be repeated. The only difference is that the amplitudes of the pattern

seem less stable against this variation, although the effect is rather small. In the Python notebook, we also repeat the analysis with a uniform distribution in the interval $[-A, A]$ rather than a Gaussian distribution from which the white noise samples are drawn. The results are almost identical, such that it appears that the choice of distribution does not alter the pattern. Hence we conclude that the system is very stable against a change of the initial conditions in general.

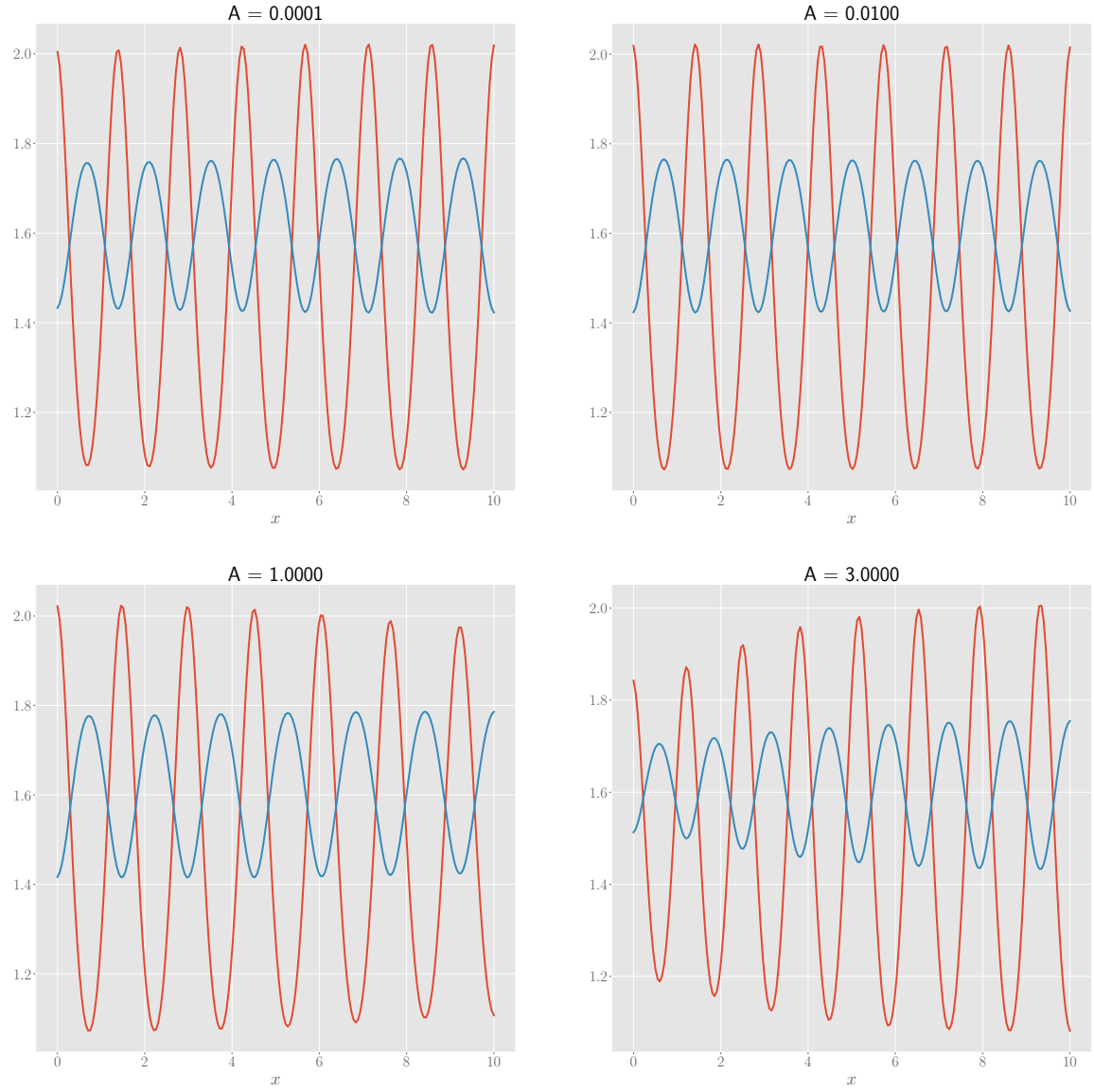

Figure 7: Varying A, the standard deviation of the Gaussian distribution, in the white noise perturbation.

3.3 Varying domain size

Figure 8 shows the effect of varying the domain size L. In the figure, we look at increasing values of L, so larger domains. We see that varying the domain size has a more significant impact compared to the variation of the initial conditions. While the shape of the pattern for $L = 15$ is similar to the one for $L = 10$, we see that the pattern for $L = 20$ has a different shape, in which the solution for u has some sort of deeper structure, where the maxima differ in height in some sort of regular way. Of course, it could be that the convergence towards the final pattern is not yet complete, hence explaining the sub-structure of the plot. However, a plot in the notebook where we integrate until $t = 10$ (compared to $t = 5$ in the figure below) gives a result which is almost identical in shape to the plot below, excluding this possibility. When we use a different initial condition, the same pattern is observed as well. Note also that the wavelength of the pattern changes if L is changed. This is due to the fact that the critical wavenumber, which has the largest real part of its growth rate and hence is expected to give the wavelength of the final pattern, depends on γ, which on itself depends on L.

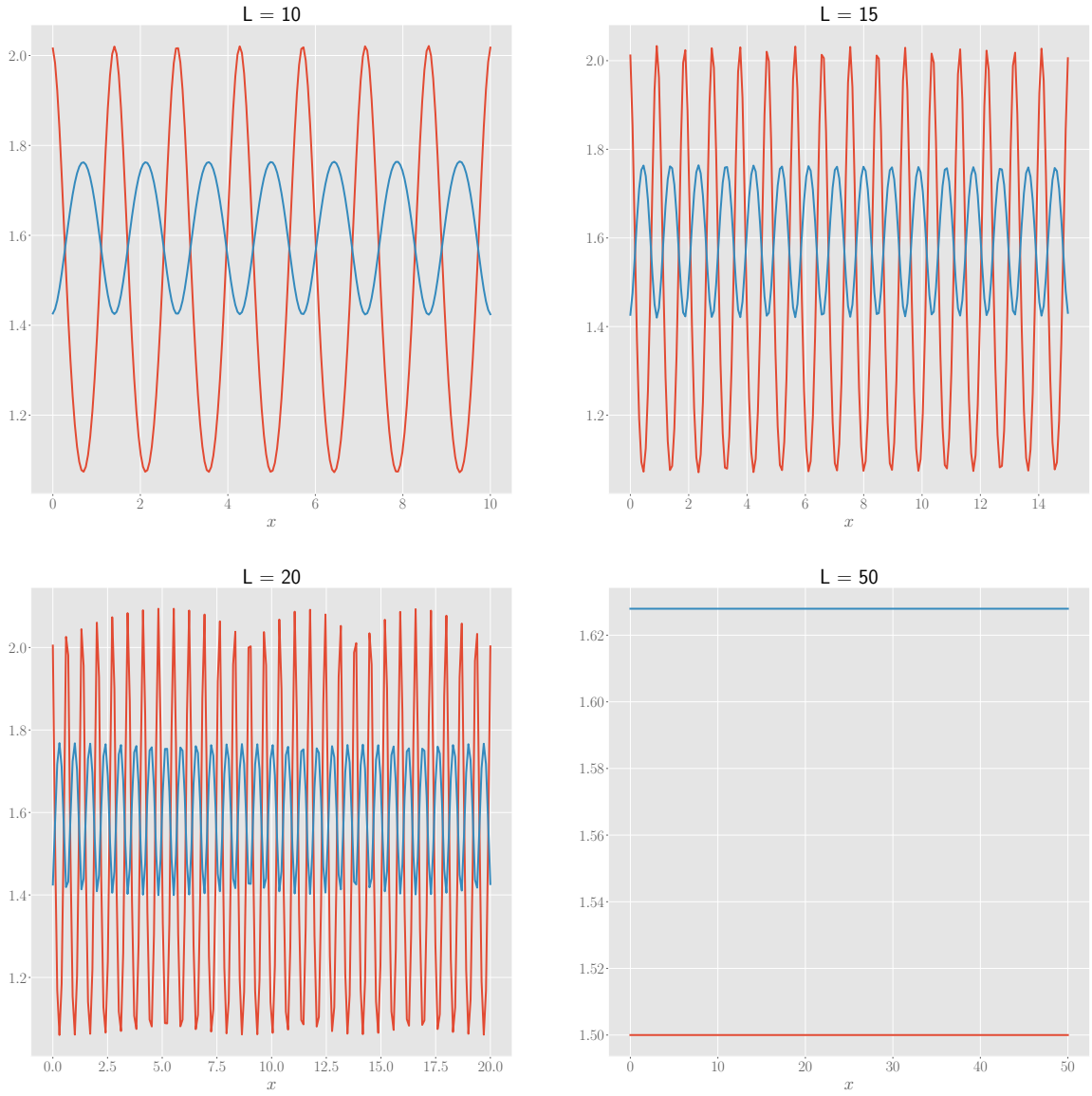

Figure 8: Varying the domain size L of the system.

Even more striking is that no pattern is formed at all for $L = 50$. In the Python notebook, we plot the solution for an initial condition with $n = 10$ (rather than $n = 1$) or where the integration time is increased to $t = 10$ (rather than $t = 5$), but still no pattern formation is observed. It seems that the pattern starts to change around $L = 20$ and gets completely disrupted for a value of L between 20 and 50. This is confirmed by Figure 9, where it is clear that for L between 20 and 30, there is still pattern formation, but the shape of the pattern becomes highly irregular (possibly because the discretization of space should be improved at higher L). For some L between 30 and 35, the system no longer tends towards a pattern solution.

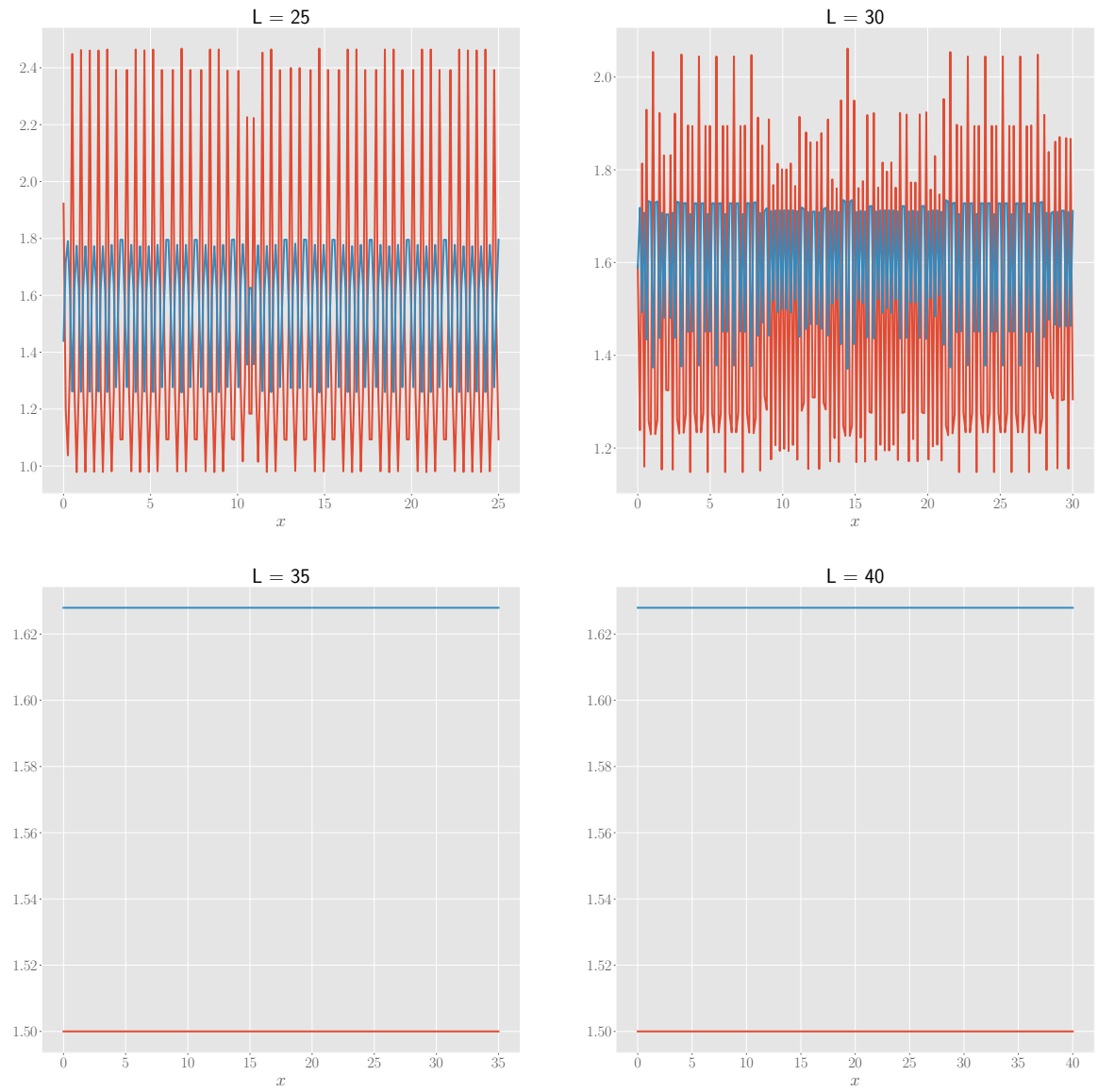

Figure 9: More variations on the domain size L, between 20 and 50, demonstrating that pattern formation stops if the domain size becomes too large.

It could be that, whereas it was unimportant for small domain sizes, the initial condition could have a significant importance for the pattern formation at large domain sizes. As observed during our analytic calculations, there is a range of unstable wavenumbers, i.e. there are bounds k_-^2, k_+^2 such that a perturbation with wavenumber $k_-^2 < k^2 < k_+^2$ is unstable. These bounds are the zeroes of $h(k^2)$, so one finds from the general formula derived in the previous section

$$k_\pm^2 = \frac{\gamma}{2d}\left[(df_u + g_v) \pm \sqrt{(df_u + g_v)^2 - 4d \det J}\right] . \tag{33}$$

These bounds are hence proportional to γ. If we compute these bounds for $L = 50$ and $b = b_c + 0.1$, we find that a sine wave perturbation with for example $n = 350$ has a wavenumber $k = n\pi/L$ which (when squared) lies between these bounds, and hence should be an unstable wave number. However, the numerical integration does not agree with this result and does not develop a pattern.

One possible explanation is the fact that the unstable wavenumbers are quantised in systems with a finite domain, with $k = n\pi/L$. Since the range of unstable wavenumbers is shifted towards large values, we need larger values for n, but this implies that the distance between unstable wavenumbers becomes larger, which possibly makes it more difficult for the system to converge towards a pattern. Another possible explanation is that k_c increases with γ (and hence L) such that the wavelength of the pattern decreases for increasing domain sizes (see for example Figure 8). It could be that if ω_c is too small, it becomes impossible for the system to self-organize into a pattern on such a small scale.

We want to stress that one should be careful in concluding that no pattern is formed at high L, since this can not be made rigorous by an analytic calculation. Moreover, we could continue the numerical exploration in the high L region, but in order to reduce computational errors, we should make our discretization of space finer, which means the calculations will take a lot of time. Hence we conclude the exploration of high domain sizes with the observation that above some L, pattern formation becomes difficult, perhaps even impossible, although this is hard to prove exactly.

Instead of extending towards higher domains, we also investigated the behaviour of the system in smaller domain sizes, i.e. with $L \leq 10$. It turns out that if the domain is too small, no patterns are formed. Contrary to the high L regime, this can be argued from an analytic point of view. Recall the range of unstable wavenumbers with bounds given by equation (33) and proportional to γ (therefore proportional to L^2). The unstable wavenumbers become quantised in finite domain systems with lowest possible wavenumber squared being π^2/L^2. Hence if L is sufficiently small, there exist no (quantised) wavenumber in the range of unstable wavenumbers, such that no pattern is formed.

References

[1] JD Murray. *Mathematical biology II: spatial models and biomedical applications*, volume 2. Springer-Verlag, 2001.